J. Membrane Biol. 210, 21–29 (2006)
DOI: 10.1007/s00232-005-7026-4

The Journal of
Membrane
Biology

Elongation of Outer Transmembrane Domain Alters Function of Miniature K^+ Channel Kcv

Brigitte Hertel[1], Sascha Tayefeh[1,2], Mario Mehmel[1], Stefan M. Kast[2], James Van Etten[3], Anna Moroni[4], Gerhard Thiel[1]

[1]Institute of Botany, University of Technology Darmstadt, Darmstadt, Germany
[2]Physical Chemistry, University of Technology Darmstadt, Darmstadt, Germany
[3]Department of Plant Pathology and Nebraska Center for Virology, University of Nebraska, Lincoln, Nebraska 8583-0722
[4]Dipartimento di Biologia, CNR-IBF & INFM: Consiglio Nazionale della Ricerche-Istituto di Biofisica e Istituto Nazionale Fisica della Material, Unità di Milano Università, Via Celoria 26, 20133, Milan, Italy

Received: 15 December 2005/Revised: 3 February 2006

Abstract. The virus-coded channel Kcv has the typical structure of a two-transmembrane domain K^+ channel. Exceptional are its cytoplasmic domains: the C terminus basically ends inside the membrane and, hence, precludes the formation of a cytoplasmic gate by the so-called bundle crossing; the cytoplasmic N terminus is composed of only 12 amino acids. According to structural predictions, it is positioned in the membrane/aqueous interface and connected via a proline kink to the outer transmembrane domain (TM1). Here, we show that this proline kink affects channel function by determining the position of TM1 in the membrane bilayer. Extension of the hydrophobic length of TM1 by either eliminating the proline kink or introducing an alanine in TM1 augments a time- and voltage-dependent inward rectification of the channel. This suggests that the positional information of TM1 in the bilayer is transmitted to a channel gate, which is not identical with the cytoplasmic bundle crossing.

Key words: K^+ channel gating — Transmembrane domain — Viral channel Kcv — Ion selectivity — Hydrophobic mismatch

Introduction

The crystal structures of several bacterial K^+ channels have provided major insight at the atomic scale into basic functional properties of these proteins (MacKinnon, 2003). The ability of the channels to select K^+ over other cations can now be understood from the architecture of the selectivity filter, where the permeant ions interact directly with backbone carbonyl oxygen atoms (Doyle et al., 1998). Analysis of crystal structures also provides some insight into the mechanism of gating, i.e., the mechanism which generates the opening and closing of ion channels. One gate is associated with a tight cytoplasmic constriction in the tetrameric protein generated by a crossing of the inner portion of the inner transmembrane domains (TM2) (Doyle et al., 1998; Jiang et al., 2002). This model is supported by data from electron paramagnetic resonance spectroscopy in which the bacterial channel KcsA undergoes rotational movements of TM2 after activation and a subsequent widening of the cytoplasmic constriction (Perozo, Cortes & Cuello, 1999). A somewhat more complex picture emerged from electron crystallographic studies on KirBac3.1 (Kuo et al., 2005). These structural data suggest that the closed/open transition is achieved by bending of the inner helices in concert with significant movements of the outer helices in order to provide access of the ions to the pore.

In addition to this intracellular gate, some authors propose a second gating mechanism that involves the selectivity filter. The existence of this additional gate is supported by several experimental and theoretical studies (Bichet et al., 2004; Domene, Grottesi & Sansom, 2004; VanDongen, 2004). Strong support for a gate in the selectivity filter also comes from investigations on the viral K^+ channel Kcv. This miniature channel protein and its homologues exhibit gating (Gazzarrini et al., 2002, 2004), even though their TM2 is too short to form a bundle crossing (Plugge et al., 2000; Gazzarrini et al., 2004; Kang et al., 2004).

Correspondence to: Gerhard Thiel; email: thiel@bio.tu-darmstadt.de

Previous findings indicated that not only the inner transmembrane domain TM2 but also TM1 is important for K^+ channel gating. Work on Kcv and its variants has demonstrated a strong impact on gating by mutation of residues expected to reside in TM1 (Gazzarrini et al., 2004). A similar role of TM1 in gating was derived from the analysis of random mutants of the G protein-coupled K^+ inward rectifier GIRK2 channel (Bichet et al., 2004). Collectively, these experiments led to the prediction that large-scale motions and/or long-range interactions between TM1 and other channel domains affect channel gating and ion permeation (Bichet et al., 2004; Gazzarrini et al., 2004).

Homology modeling of the viral channel Kcv on the KirBac1.1 structure suggests that the structure of the viral channel resembles that of bacterial channels (Doyle et al., 1998; Kuo et al., 2003). This similarity includes the presence and position of the main pore module elements such as pore helix, selectivity filter, turret and transmembrane domains (Gazzarrini et al., 2004). Also, a helical domain reminiscent of the "slide helix" in KirBac1.1 (Kuo et al., 2003) upstream of TM1 at the membrane/water interface seems to be present in Kcv and to correspond to the 12-amino acid putative cytosolic N terminus of the channel. Because of these overall structural similarities with other K^+ channels, the miniature viral channel presents a suitable model system for understanding basic structure and function correlates in the pore module of K^+ channels.

In the present study, we used the miniature viral K^+ channel Kcv to examine the role of the outer transmembrane domain (TM1) on channel function. Our results show that manipulations which increase the effective hydrophobic length of TM1 promote a time- and voltage-dependent inward rectification of the Kcv channel in HEK293 cells. Since transmembrane domains have to avoid a mismatch in their length with respect to the bilayer thickness (Killian & von Heijne, 2000), the data are compatible with the view that the orientation of TM1 in the lipid bilayer plays a role in channel function.

Materials and Methods

Mutagenesis and Transfection of Mammalian Cell Lines

The Kcv gene was cloned into the BgIII and EcoRI sites of the pEGFP-N2 eukaryotic expression vector (Clontech, Palo Alto, CA) in frame with the downstream enhanced green fluorescent protein (EGFP) gene by deleting the Kcv stop codon.

Point mutations were created by the QuikChange method (Stratagene, La Jolla, CA) and confirmed by sequencing. For functional expression, HEK293 cells were transfected with wild-type (wt) Kcv::EGFP or Kcv mutants. The plasmid pEGFP-N2 containing the EGFP gene only was used for mock transfection of control cells. HEK293 cells were transiently transfected using the liposomal transfection reagent metafectene (Biontex Laboratories, Munich, Germany).

Electrophysiology

Experiments were performed on cells incubated after transfection at 37°C in 5% CO_2 for 2-3 days. On the day before the experiment, cells were dispersed by trypsin, plated at a low density on 35 mm culture dishes and allowed to settle overnight. Dishes were then placed on the stage of an inverted microscope, and single cells were patch-clamped in the whole-cell configuration according to standard methods (Hamill et al., 1981) using an EPC-9 patch-clamp amplifier (HEKA, Lambrecht, Germany). Data acquisition and analysis were performed using Pulse software (HEKA).

Cells were perfused at room temperature with a control solution containing 100 mM KCl, 1.8 mM $CaCl_2$, 1 mM $MgCl_2$ and 5 mM 4-(2-hydroxyethyl)-1-piperazineethanesulfonic acid (HEPES, pH 7.4). Choline-Cl was used to adjust the osmolarity to 300 mOsmol. Fast delivery of the solution was obtained with a perfusion pipette positioned on top of the cell under study, which allowed relatively rapid solution changes. Whole-cell pipettes contained 130 mM D-potassium-gluconic acid, 10 mM NaCl, 5 mM HEPES, 0.1 mM guanosine triphosphate (Na salt), 0.1 μM $CaCl_2$, 2 mM $MgCl_2$, 5 mM phosphocreatine and 2 mM adenosine triphosphate (Na salt, pH 7.4).

Modeling of Kcv and Mutants

Three-dimensional coordinates of Kcv-wt were obtained by homology modeling using the X-ray structure of Kirbac3.1 (PDB entry 1P7B) as template. This procedure was followed by energy minimization and vacuum molecular dynamics (MD) relaxation. The alignment procedure was described in more detail by Gazzarrini et al. (2004), taking into account the suggestions by Durell & Guy (1999). Homology modeling was performed using Modeller v6.2 (Marti-Renom et al., 2000). The resulting tertiary structures were evaluated using ProsaII (Sippl, 1993) and Procheck (Laskowski et al., 1993). Rotational symmetry was imposed, followed by energy minimization using rigid constraints for potassium ions, strong harmonic restraints for all nonproton atoms of filter residues 61-69 and weaker harmonic restraints for N-terminal C-α atoms. An MD run in vacuo of approximately 5 ns was performed in order to probe the structural stability. During an equilibration period, harmonic restraints for all C-α atoms were gradually removed over a period of 330 ps. Filter residues 63-67 and potassium ions in the filter region were kept rigid to avoid uncontrolled monomer dislocation. Both energy minimization and MD simulations were performed with the academic version of Charmm 3.1b1 (Brooks et al., 1983). Final visualization of the monomers, which are shown in Figure 1*B* and *C*, were generated with Molcad (Brickmann et al., 1995).

The Kcv-P13A mutant could not be modeled using the unmodified Kirbac3.1 structure template because alanine is known to stabilize a helical structure rather than to interrupt helical symmetry, as expected from proline. Thus, an ideal α-helix for Kcv-P13A residues 1-16 was created with Sybyl 6.9 (Tripos, St. Louis, MO).

Three C-terminal residues were superimposed onto corresponding residues of the Kcv-wt model, followed by the same procedure described above.

The structural predictions for the proteins were obtained with the following five independent algorithems: PROF (http://bioinf.cs.ucl.ac.uk/psipred/), NNPREDICT (www.cmpharm.ucsf.edu/~nomi/nnpredict.html), SOPMA (http://npsa-pbil.ibcp.fr/cgi-bin/npsa_automat.pl?page=/NPSA/npsa_server.html), PSIPRED (http://www.aber.ac.uk/~phiwww/prof/), PREDATOR (http://www-db.embl-heidelberg.de/jss/servlet/de.embl.wwwTools.GroupLeftEMBL)

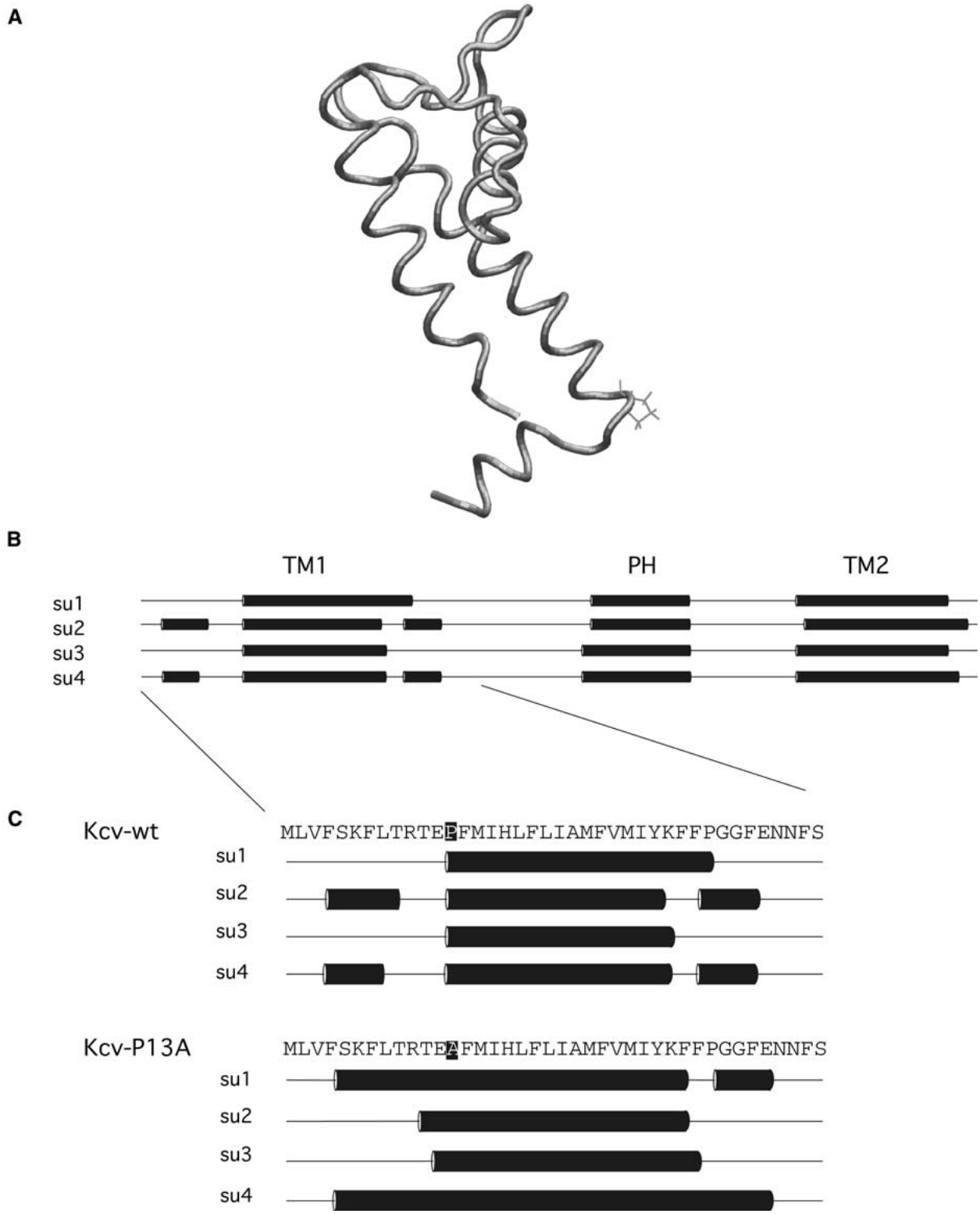

Fig. 1. Model predictions for Kcv channel. (*A*) Kcv monomer with indication of P^{13} position. The structure was obtained by homology modeling of Kcv on KirBac3.1 structure and subsequent energy minimization. (*B*) Predictions for secondary structure of Kcv-wt. The locations of ideal α-helices are indicated by *solid bars* in the four subunits (su1-su4); they correspond to the two transmembrane domains (TM1, TM2) and the pore helix (PH) of Kcv-wt channel. Ideal α-helices were identified according to criteria of Frishman & Argos (1995) by analyzing the Kcv model following 5 ns of partially constrained MD run *in vacuo*. (*C*) Enlargement of secondary structure predictions from MD run for N-terminal 40 amino acids in Kcv-wt and Kcv-P13A mutant. Position 13 is highlighted in both sequences.

Fig. 2. Predictions of secondary structure for Kcv-wt and mutants in position P^{13}. This position is highlighted in the sequences. The structural predictions for the wt and mutant channels were obtained with five independent algorithms (PROF, NNPREDICT, SOPMA, PSIPRED, PREDATOR) indicated on the right (for details, see Materials and Methods). A consensus per-residue prediction was derived if three or more of the different softwares (black letters) or two (gray letters) provided the same secondary structure. *H*, α-helix; *E*, β-sheet; *C*, coil; -, not assigned.

Results

Homology modeling of Kcv on the structure of KirBac1.1 illustrates the overall architecture of the viral channel shown in Figure 1*A*. A prominent position in this structure is Pro^{13}. As in KirBac1.1 (Kuo et al., 2003), this amino acid marks the beginning of the α-helix, which forms the outer transmembrane domain (TM1). Furthermore, because of the structural repercussions of Pro imposing a kink in an amino acid chain (Cordes, Bright & Sansom, 2002; Labro et al., 2003), the structure exhibits in this position an angle between the cytosolic N terminus and TM1.

To examine the role of Pro^{13} in structure and function of Kcv, the amino acid was replaced by Ala, the amino acid with the highest propensity for helix formation (O'Neil & DeGrado, 1990). Several structural prediction algorithms suggest that the α-helix of TM1 starts with Pro^{13} (Fig. 2). The same algorithms predict that a mutation of Pro^{13} into Ala results in an extension of the TM1 α-helix (Fig. 2). To obtain further independent information on the secondary structures of TM1 in the context of the whole tetrameric channel, we also monitored its architecture in an MD run in vacuo. The resulting equilibrated structure was analyzed with respect to its secondary structure using an algorithm developed by Frishman & Argos (1995). The data in Figure 1*B* show the location of ideal α-helices in the channel in representative snapshots of a structure from the equilibrated ensemble; the pore loop and the two transmembrane domains exhibit, as expected, stable α-helices. Similar to the prediction algorithms also, the MD simulation marks Pro^{13} as the start of the TM1 α-helix. The simulation shows further that replacing Pro^{13} by Ala (Kcv-P13A) promotes the tendency of the TM1 α-helix to elongate (Fig. 1*C*). Hence, both MD simulations and structural prediction algorithms propose that replacement of Pro^{13} with Ala results in an extension of the TM1 α-helix by two or more amino acids. Worth noting is that preliminary data from MD simulations of a fully solvated, lipid-embedded model agree with this suggestion (S. Tayefeh, A. Moroni, G. Thiel, S. M. Kast, unpublished data).

To examine the effect of substituting Pro^{13} by Ala on channel function, wt and mutant (Kcv-P13A) channels were expressed in HEK293 cells. Figure 3*A* shows for reference the current responses of a HEK293 cell transfected with EGFP to a standard pulse protocol (holding voltage 0 mV, 800 ms test voltages between +60 and −160 mV). These cells produce the typical background conductance of HEK293 cells with a low conductance at negative clamp voltages and a small K^+ outward rectifier at

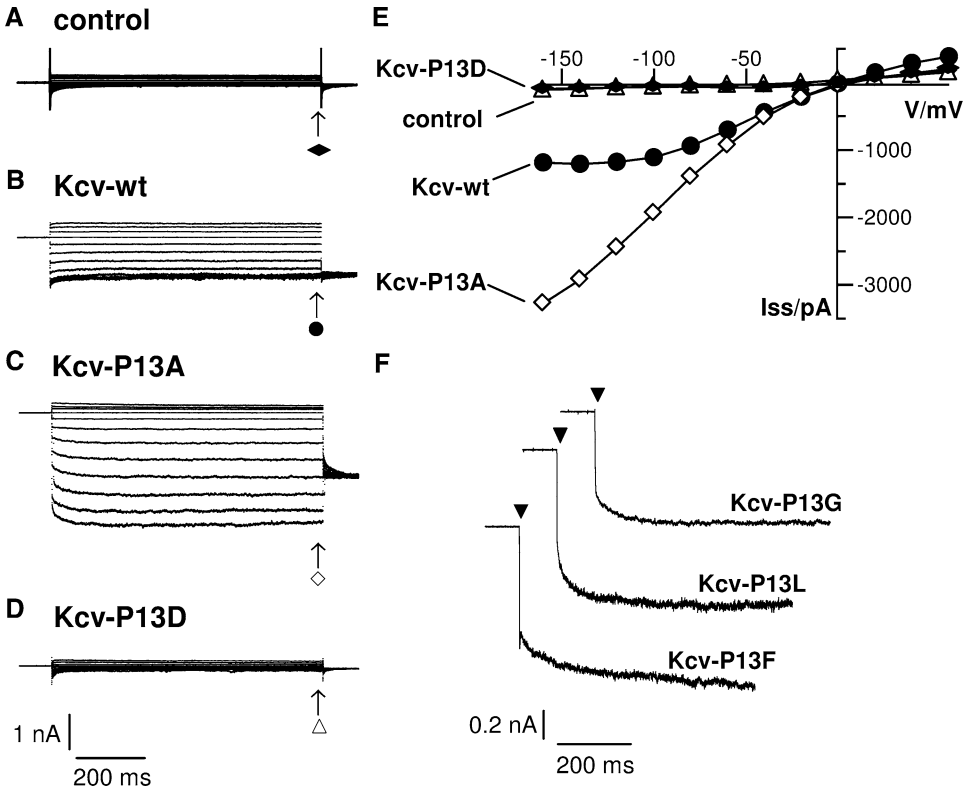

Fig. 3. Mutation of Pro^{13} has drastic effects on Kcv channel function. (*A-D*) Current responses of HEK293 cells transfected with GFP (*A*), Kcv-wt (*B*), Kcv-P13A (*C*) or Kcv-P13D (*D*) to standard voltage protocol from holding voltage (0 mV) to test voltages between +60 and −160 mV. (*F*) Current response of HEK293 cells transfected with mutant channels to voltage steps from a holding voltage of 0 to −160 mV. (*E*) Steady-state I/V relations of currents in (*A-D*); symbols cross-reference with symbols in (*A-D*).

positive voltages (Fig. 3*A* and *E*). In these control cells, the ratio of slope conductance at negative voltages (−20 to −60 mV, G_{neg}) *vs.* conductance at positive voltages (0 to +60 mV, G_{pos}) was always less than 1. Cells transfected with a chimera of Kcv and GFP (Kcv-wt; all constructs in this study are chimeras with GFP linked to the C terminus; for simplicity, GFP is not included in the channel name) often exhibit an additional large inward current with typical features. A representative example of this current and the corresponding current/voltage(I/V) relation is shown in Figure 3*B* and *E*; a characteristic of this conductance is that it increases linearly with clamp voltage between 0 and about −80 mV. At more negative voltages, the conductance passes a maximum. It was previously shown that the Kcv::GFP chimera generates a conductance in HEK293 cells with these features (Moroni et al., 2002). In contrast to the control cells, the ratio of G_{neg}/G_{pos} in cells with Kcv conductance is always larger than 1. Using a ratio of $G_{neg}/G_{pos} \geq 1$ as a parameter for Kcv activity, we estimated a fractional expression of the channel of about 65% in GFP fluorescent HEK293 cells.

The Kcv-P13A mutant conducts a clearly different current (Fig. 3*C* and *E*). Clamp voltages more negative than −40 mV always resulted in a biphasic current response. At more negative voltages, a slow time- and voltage-dependent component was superimposed on an instantaneous current. Further scrutiny of the current responses also revealed a difference in the instantaneous current compared to the wt channel. I/V plots show that the instantaneous current (Ii) from Kcv-wt channels has a characteristic voltage-dependent decrease at negative clamp voltages (Fig. 4). In contrast, the decrease in current is shifted to more negative voltages in the Kcv-P13A mutant (Fig. 4). In addition to these kinetic differences, the total current of cells expressing Kcv-P13A was higher than in cells expressing Kcv-wt (Fig. 5). Student's *t*-test indicated that the difference in current at −140 mV in Kcv-wt and Kcv-P13A expressing cells is significant ($P > 0.04$).

To examine the impact of the P13A mutation on the general features of channel function, we also examined the ability of the channels to discriminate between K^+ and Na^+ and their susceptibility to Ba^{2+} block. The data summarized in Table 1 show that Kcv-P13A exhibits the same sensitivity to Ba^{2+} as wt-Kcv. On the other hand, the negative shift of the reversal voltage following a complete exchange of K^+ to Na^+ in the bath solution is more pronounced than in wt channels. This result indicates that Kcv-P13A is more selective than wt-Kcv.

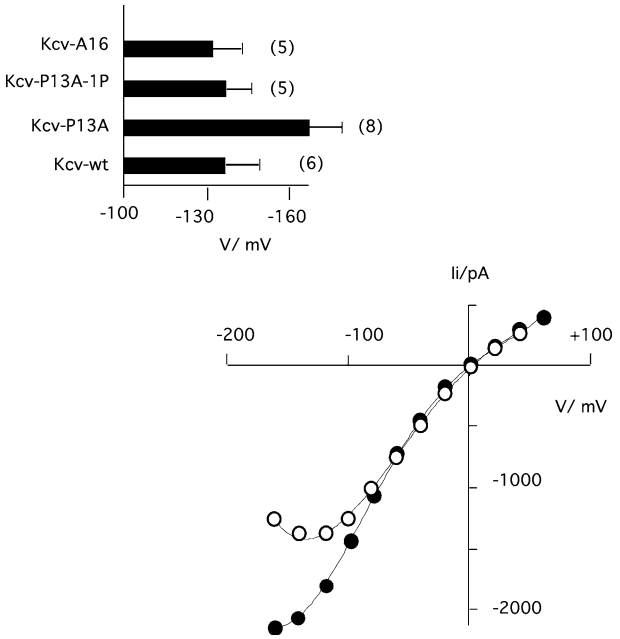

Fig. 4. Voltage dependence of instantaneous current (Ii) in Kcv-wt and mutant channels. Instantaneous current Ii/V relation of HEK293 cells expressing Kcv-wt (*open symbols*) or Kcv-P13A (*closed symbols*) channel. Currents were obtained 3 ms after stepping cell from folding voltage to a range of test voltages. Ii/V data were fitted with fourth-order polynomial (*lines*). *Inset*: Mean voltages (± standard deviation) at which the first derivative of the polynomial fit is zero. *n*, number of cells analyzed.

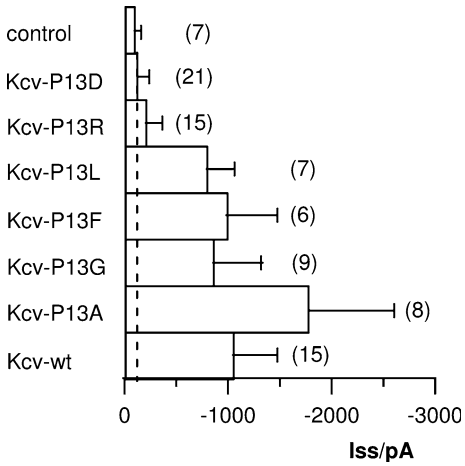

Fig. 5. Mean steady-state current (± standard deviation) of Kcv currents at −100 mV in HEK293 cells transfected with GFP (control), Kcv-wt channel or the mutant channels. Number of recordings indicated in parentheses.

It is interesting that channels with the same characteristics, i.e., with a time-dependent component (Fig. 3*F*) and quasi-linear I/V relation of steady-state current, albeit with a lower current density (Fig. 5), were obtained when Pro^{13} was replaced with an amino acid with a lower helix-forming tendency (e.g., Phe or Leu) (O'Neil & DeGrado, 1990). Also, replacing Pro^{13} with Gly, an amino acid which destabilizes the α-helical configuration (O'Neil & DeGrado, 1990) and in principle allows the structure to adopt the proline configuration, produced channels with similar characteristics (Fig. 3*F*). These data are consistent with the structural predictions, which indicate that these amino acid substitutions might result in an elongation of the TM1 α-helix (Fig. 2).

Worth noting is that the position of Pro^{13} does not tolerate all amino acid exchanges; when Pro^{13} was exchanged with the charged amino acids Arg (R) or Asp (D), no channel conductance was measurable (Fig. 5). The resulting currents were identical to those from mock-transfected cells (Fig. 3*D* and *E*).

Position of Proline

The results establish that Pro^{13} plays an essential role in Kcv function. It is consistent with the view that Pro^{13} forces a kink in the structure, which determines the positioning of the N terminus in the membrane/cytoplasm interface. To examine further the role of Pro, this amino acid was also reintroduced into the functional Kcv-P13A mutant. Pro was inserted either one amino acid upstream (−1P) or downstream (+1P) of the original position. The data show that the +1P mutant basically restores the Kcv-wt kinetics (compare Fig. 6*A* and *D*). Hence, an elongation of the protein by an Ala upstream of Pro^{13} has no effect on channel performance.

In contrast, introduction of a Pro at position −1 in the Kcv-P13A mutant produced a mixed phenotype (Fig. 6*B* and *D*). The channel still contained a significant time-dependent component, but while the time-dependent component of Kcv-P13A-1P was similar to that of the Kcv-P13A mutant (Fig. 6*D*), the two channels differed in the voltage dependence of the instantaneous current (Fig. 4). Other than Kcv-P13A, this mutant reveals a stronger inhibition of the steady-state and instantaneous current at negative voltages. Hence, extension of TM1 downstream of Pro^{13} results in a general gain of channel activity; it introduces a time-dependent inward rectifying kinetic component of the channel.

The results obtained with Kcv-P13A-1P imply that it is not the removal of the proline but rather the extension of the TM1 that probably generates the time-dependent component of the current in Kcv. To further examine if the gain of function in Kcv-P13A-1P is related to TM1 extension, a mutant, Kcv-A16, was constructed on the basis of the wt channel in which an additional Ala was introduced in position 16 in Kcv-wt. Testing channel function revealed that this modification also caused an inward current with a time-dependent component (Fig. 6*C*). The features of this mutant are similar to

Table 1. Sensitivity of Kcv-wt and Kcv-P13A channel to Ba^{2+} block and K^+/Na^+ selectivity[a]

Channel	Ba^{2+} block at −140 mV (%)	V_{rev}/mV in 100 mM K^+	V_{rev}/mV in 100 mM Na^+	ΔV_{rev}/mV
Kcv	85.0 ± 10.6 (n = 6)	5 ± 0 (n = 5)	−61 ± 9 (n = 5)	66 ± 9
Kcv-P13A	89.7 ± 9.4 % (n = 4)	2 ± 1 (n = 5)	−89 ± 7 (n = 5)	90 ± 7

[a] The current responses of HEK293 cells expressing Kcv-wt, ΔN7-Kcv or Kcv-P13A were measured as in Figures 5 and 6 before and after addition of 10 mM Ba^{2+} to bath medium and after replacing 100 mM K^+ for 100 mM Na^+ in bath medium. The Ba^{2+} block was estimated as relative decrease of the current at −140 mV in the absence and presence of inhibitor. The relative selectivity of the channels for K^+ over Na^+ was estimated from the shift of the reversal voltage (V_{rev}) due to the exchange of cations. Data are mean values ± standard deviation from n experiments.

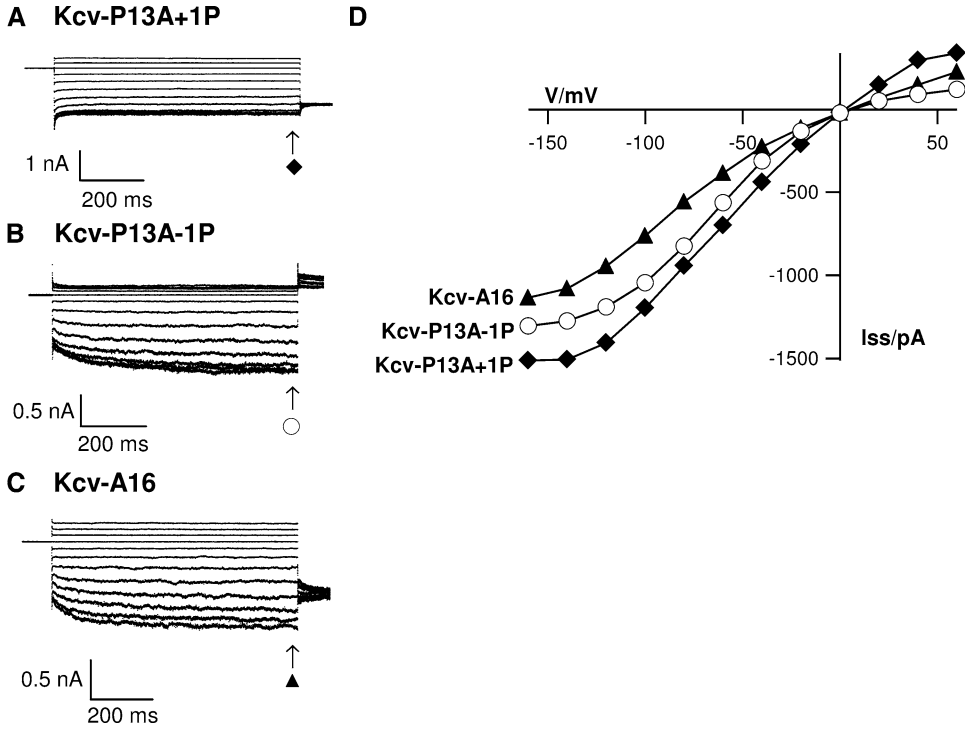

Fig. 6. Introduction of Ala in N-terminal part of Kcv affects channel function depending on whether the amino acid is introduced upstream or downstream of Pro^{13}. Current responses of HEK293 cells transfected with (*A*), Kcv-P13A + 1P, (*B*) Kcv-P13A-1P or (*C*) Kcv-A16 to standard voltage protocol from holding voltage (0 mV) to test voltages between +60 and −160 mV. (*D*) Steady-state I/V relations of currents in (*A-C*); symbols cross-reference with symbols in (*A-C*).

those produced by Kcv-P13A-1P (Figs. 4, 6*B* and *C*). Thus, an extension of TM1, irrespective of whether this is done near or far from the Pro, results in a time-dependent component.

Discussion

The Effective Hydrophobic Length of TM1 on Channel Function

The present study examined structure/function correlates in a chimera of the viral channel Kcv and a C-terminally linked GFP. The key observation is that extension of the outer transmembrane domain (TM1) of Kcv has substantial effects on the activity of this channel. The occurrence of a time-dependent inward rectifying component of the channel in HEK293 cells was promoted by any extension of TM1. This stimulating effect was independent on the positions at which it was extended as long as the extension was within the transmembrane domain. In contrast to this, an extension of the protein upstream of Pro^{13} did not affect activity. These observations stress that the activity of the channel is influenced by the effective length of TM1 with respect to the lipid bilayer.

The present data are consistent with previous findings indicating that TM1 is important in K^+ channel gating. Work on Kcv and its variants has already shown that modifications in the TM1 domain can have drastic impacts on channel gating (Gazzarrini et al., 2004). Similar conclusions resulted

from analysis of random mutants of the G protein-coupled inward rectifier GIRK2 channel (Bichet et al., 2004). These experiments led to the prediction that large-scale motions and/or long-range interactions between TM1 and other channel domains affect channel gating and ion permeation (Bichet et al., 2004; Gazzarrini et al., 2004). Since Kcv apparently has no other gate than the selectivity filter (Gazzarrini et al., 2004), any changes in TM1 length have to be translated into a conformational change inside the pore region. It is tempting to speculate that any movement of TM1 in Kcv is coupled directly or indirectly via a salt bridge to adjacent structural domains in the pore. Such a functional coupling between a TM domain and the selectivity filter is, for example, known for the Shaker channel (e.g., Ogielaska & Aldrich, 1998). In this regard, the present results are consistent with the hypothesis that TM1 interferes indirectly with permeation and gating processes in the pore. The proposed movement of TM1 has indeed been detected from the analysis of conformational rearrangements of the KcsA channel during pH-dependent gating. Spectroscopic data suggested a significant rotational movement of TM1 with most of the tilt toward the N-terminal end (Perozo et al., 1999). Also, in the bacterial channel KirBac3.1, it was found that open/closed transitions of the channel are associated with appreciable movements of the outer transmembrane domain (Kuo et al., 2005).

In the context of the Kcv structure, an extension of TM1 has implications for the positioning of this domain in the bilayer. Scrutiny of TM1 shows that it has the typical structure of a transmembrane protein (dePlanque & Killian, 2003; Hessa et al., 2005) in the sense that the boundaries on both sides are determined by charged amino acids. In the case of Kcv, TM1 is flanked on the cytoplasmic/membrane interphase by a Glu (E^{12}). This negatively charged amino acid can be expected to be repelled by the negatively charged phosphate groups in the bilayer (Killian & von Heijne, 2000). On the external lipid/water interface, TM1 reveals a positively charged Lys (K^{29}, Figs. 1 and 2); this amino acid has been shown to determine the positioning of transmembrane proteins in the lipid/water interface (Killian & von Heijne, 2000). As a repercussion, it can be assumed that the positioning of TM1 in the lipid bilayer and, in particular, the relevant hydrophobic length are well defined by the distance between the two charged amino acids (Killian & von Heijne, 2000; Hessa et al., 2005). Any increase in the length of TM1 between the charges will produce a hydrophobic mismatch and thus force TM1 into a different conformation in the bilayer (Killian & von Heijne, 2000). It has been shown previously that such conformational rearrangements in the protein/bilayer mismatch can influence the activity of transport proteins (Dumas, Lebrun & Tocanne, 1999); a well-studied example is the gating of stretch-activated channels (Perozo et al., 2002). The present results suggest that a conformational change in TM1 due to a rearrangement of the protein in the lipid bilayer is also involved in the function of viral K^+ channel Kcv.

The present data have implications in understanding the function of more complex K^+ channels. The data imply that any mechanical dislocation of TM1 on the atomic scale can result in a modification of channel activity. This could provide a mechanism by which a conformational change of the cytoplasmic N terminus [e.g., as a result of ligand binding or movement of voltage sensor in voltage-gated (K_V) channels] is transmitted into a modification of channel gating. Hence, movement of the S4 domain in six-transmembrane domain channels may be converted into a gating of the channel pore via displacement not only of the inner transmembrane (Long, Campbell & MacKinnon, 2005) but also of the outer transmembrane domain.

We are grateful to Rikard Blunck (Los Angeles) and Antoinette Killian (Utrecht) for helpful discussions. We also thank Jack Dainty (Norwich) for help with the manuscript. Particular thanks to Gisela Marx for excellent technical assistance. This work was supported in part by the Deutsche Forschungsgemeinschaft (to G. T. and S. M. K.); Fonds der Chemischen Industrie and the Adolf-Messer-Stiftung (to S. M. K.); the Ministero Istruzione Università e Ricerca, Progetto Fondo per gli Investimenti della Ricerca di Base (to A. M.); National Institutes of Health grant GM32441 (to J. V. E.); and grant P20RR15635 from the COBRE Program of the National Center for Research Resources (to J. V. E.).

References

Bichet, D., Lin, Y., Ibarra, C.A., Huang, C.S., Yi, B.A., Jan, Y.N., Jan, L.Y. 2004. Evolving potassium channels by means of yeast selection reveals structural elements important for selectivity. *Proc. Natl. Acad. Sci. USA* **101:**4441–4446

Brickmann J., Goetze T., Heiden W., Moeckel G., Reiling S., Vollhardt H., Zachmann C.D. 1995. Data visualization in molecular science. *In:* J.D. Bowie, ed. Tools for Insight and Innovation, Addison-Wesley, Reading, PA pp 83-97.

Brooks, B.R., Bruccoleri, R.E., Olafson, B.D., States, D.J., Swaminathan, S., Karplus, M. 1983. CHARMM: A program for macromolecular energy minimization and dynamics calculations. *J. Comput. Chem.* **4:**187–217

Cordes, F.S., Bright, J.N., Sansom, M.S.P. 2002. Proline-induced distortions of transmembrane helices. *J. Mol. Biol.* **323:**951–960

dePlanque, M.R.R., Killian, J.A. 2003. Protein-lipid interactions studied with designed transmembrane peptides: Role of hydrophobic matching and interfacial anchoring. *Mol. Membr. Biol.* **20:**271–284

Domene, C., Grottesi, A., Sansom, M.S.P. 2004. Filter flexibility and distortion in a bacterial inward rectifier K^+ channel: Simulation studies of KirBac1.1. *Biophys. J.* **87:**256–267

Doyle, D.A., Cabral, J.M., Pfuetzner, R.A., Kuo, A., Gulbis, J.M., Cohen, S.L., Chait, B.T., MacKinnon, R. 1998. The structure of the potassium channel: Molecular basis of K^+ conduction and selectivity. *Science* **280:**69–76

Dumas, F., Lebrun, M.C., Tocanne, J.F. 1999. Is the protein/lipid hydrophobic matching principle relevant to membrane organization and function? *FEBS Lett.* **58:**271–277

Durell, S.R., Guy, H.R. 1999. Structural models of the KtrB, TrkH, and Trk1,2 symporters based on the structure of the KcsA K^+ channel. *Biophys. J.* **77:**789–807

Frishman, D., Argos, P. 1995. Knowledge-based secondary structure assignment. *Proteins* **23:**556–579

Gazzarrini, S., Kang, M., Van Etten, J.L. Van , Tayefeh, S., Kast, S.M., DiFrancesco, D., Thiel, G., Moroni, A. 2004. Long-distance interactions within the potassium channel pore are revealed by molecular diversity of viral proteins. *J. Biol. Chem.* **279:**28443–28449

Gazzarrini, S., Van Etten, J.L., DiFrancesco, D., Thiel, G., Moroni, A. 2002. Voltage-dependence of virus encoded miniature K^+-channel Kcv. *J. Membr. Biol.* **187:**15–25

Hamill, O.P., Marty, A., Neher, E., Sakmann, B., Sigworth, F. 1981. Improved patch-clamp techniques for high-resolution current recording from cells and cell-free membrane patches. *Pfluegers Arch.* **391:**85–100

Hessa, T., Kim, H., Bihlmaier, K., Lundin, C., Boeckel, J., Andersson, H., Nilsson, I.M., White, S.H., von Heijne, G. 2005. Recognition of transmembrane helices by endoplasmic reticulum translocon. *Nature* **433:**377–382

Jiang, Y., Lee, A., Chen, J., Cadene, M., Chait, B.T., MacKinnon, R. 2002. Structure and mechanism of a calcium-gated potassium channel. *Nature* **417:**515–522

Kang, M., Moroni, A., Gazzarrini, S., DiFrancesco, D., Thiel, G., Severino, M., Van Etten, J.L. 2004. Small potassium ion channel proteins encoded by chlorella viruses. *Proc. Natl. Acad. Sci. USA* **101:**5318–5324

Killian, J.A., von Heijne, G. 2000. How proteins adapt to a membrane-water interface. *Trends Biochem. Sci.* **25:**429–434

Kuo, A., Domene, C., Johnson, L.N., Doyle, D.A., Vénien-Bryan, C. 2005. Two different conformational states of the KirBac3.1 potassium channel revealed by electron crystallography. *Structure* **13:**1463–1472

Kuo, A., Gulbis, J.M., Antcliff, J.F., Rahman, T., Lowe, E.D., Zimmer, J., Cuthbertson, J., Ashcroft, F.M., Ezaki, T., Doyle, D.A. 2003. Crystal structure of the potassium channel KirBac1.1 in the closed state. *Science* **300:**1922–1926

Labro, A.J., Raes, A.L., Bellens, I., Ottschytsch, N., Snyders, D.J. 2003. Gating of *Shaker*-type channels requires the flexibility of S6 caused by pralines. *J. Biol. Chem.* **278:**50724–50731

Laskowski, R.A., MacArthur, M.W., Moss, D.S., Thornton, J.M. 1993. PROCHECK: A program to check the stereochemical quality of protein structures. *J. Appl. Cryst.* **26:**283–291

Long, S.B., Campbell, E.B., Mackinnon, R. 2005. Voltage sensor of Kv1.2: Structural basis of electromechanical coupling. *Science* **309:**903–908

MacKinnon, R. 2003. Potassium channels. *FEBS Lett.* **555:**62–65

Marti-Renom, M.A., Stuart, A.C., Fiser, A., Sanchez, R., Melo, F., Sali, A. 2000. Comparative protein structure modeling of genes and genomes. *Annu. Rev. Biophys. Biomol. Struct.* **29:** 291–325

Moroni, A., Viscomi, C., Sangiorgio, V., Pagliuca, C., Meckel, T., Horvath, F., Gazzarrini, S., Valbuzzi, P., Van Etten, J.L., DiFrancesco, D., Thiel, G. 2002. The short N-terminus is required for functional expression of the virus-encoded miniature K^+ channel Kcv. *FEBS Lett.* **530:**65–69

Ogielska, E.M., Aldrich, R.W. 1998. A mutation in S6 of Shaker potassium channels decreases the K^+ affinity of an ion binding site revealing ion-ion interactions in the pore. *J. Gen. Physiol.* **112:**243–257

O'Neil, K.T., DeGrado, W.F. 1990. A thermodynamic scale for the helix-forming tendencies of the commonly occurring amino acids. *Science* **250:**646–651

Perozo, E., Cortes, D.M., Cuello, L.G. 1999. Structural rearrangements underlying K^+-channel activation gating. *Science* **285:**73–78

Perozo, E., Cortes, D.M., Sompornpisut, P., Kloda, A., Martinac, B. 2002. Open channel structure of MscL and the gating mechanism of mechanosensitive channels. *Nature* **418:**942–948

Plugge, B., Gazzarrini, S., Nelson, M., Cerana, R., Van Etten, J.L., Derst, C., DiFrancesco, D., Moroni, A., Thiel, G. 2000. A potassium ion channel protein encoded by chlorella virus PBCV-1. *Science* **287:**1641–1644

Sippl, M.J. 1993. Recognition of errors in three-dimensional structures of proteins. *Proteins* **17:**355–362

VanDongen, A.M.J. 2004. K channel gating by an affinity-switching selectivity filter. *Proc. Natl. Acad. Sci. USA* **101:** 3248–3252